Biomed Microdevices (2010) 12:41–48
DOI 10.1007/s10544-009-9356-y

Microtube-based electrode arrays for low invasive extracellular recording with a high signal-to-noise ratio

Kuniharu Takei · Takeshi Kawano · Takahiro Kawashima · Kazuaki Sawada · Hidekazu Kaneko · Makoto Ishida

Published online: 15 September 2009

Abstract We report on the development of a microtube electrode array as a neural interface device. To combine the desired properties for the neural interface device, such as low invasiveness with a small needle and a good signal-to-noise ratio in neural recordings, we applied the structure of a glass pipette electrode to each microtube electrode. The device was fabricated as sub-5-μm-diameter out-of-plane silicon dioxide microtube arrays using silicon microneedle templates, which are grown by the selective vapor–liquid–solid method. The microtubes had inner diameters of 1.9–6.4 μm and a length of 25 μm. Impedances ranged from 220 kΩ to 1.55 MΩ, which are less than those for conventional microneedles. In addition, the microtube electrodes had less signal attenuation than conventional microneedle electrodes. We confirmed that the effects of parasitic capacitances between neighboring microtubes and channels were sufficiently small using a test signal. Finally, neural responses evoked from a rat peripheral nerve were recorded *in vivo* using a microtube electrode to confirm that this type of electrode can be used for both electrophysiological measurements and as a neural interface device.

Keywords Microtube · Microneedle · Array · Extracellular recording · Low invasiveness · High signal-to-noise ratio

K. Takei (✉) · T. Kawano · K. Sawada · M. Ishida
Department of Electrical and Electronic Engineering,
Toyohashi University of Technology,
1-1 Hibarigaoka Tempaku-cho,
Toyohashi, Aichi 441-8580, Japan
e-mail: takei@dev.eee.tut.ac.jp

T. Kawashima
Department of Production Systems Engineering,
Toyohashi University of Technology,
1-1 Hibarigaoka Temaku-cho,
Toyohashi, Aichi 441-8580, Japan

H. Kaneko
National Institute of Advanced Industrial Science
and Technology (AIST),
1-1 Higashi,
Tsukuba, Ibaraki 305-8566, Japan

1 Introduction

Since 1970, a large number of multiple micro-fabricated electrode arrays have been used to record neural activity (Wise et al. 1970; Campbell et al. 1991). These devices have played an important role in understanding neural behavior and neuronal networks (Hochberg et al. 2006; Kawano et al. 2004; Wise et al. 2004; Ludwig et al. 2009; Kim et al. 2009). A micro-fabricated needle electrode array was implanted as a cortical neural prosthesis into the human brain of a male patient with a transected spinal cord, enabling a computer cursor and an artificial hand to be controlled at will by this patient (Hochberg et al. 2006).

Compared to classical recording methods such as metal electrodes, various out-of-plane penetrating microneedle electrode structures have been proposed to minimize invasiveness and increase spatial resolution (Hochberg et al. 2006; Kawano et al. 2004; Fitzsimmons et al. 2007). The reported microneedle arrays have been manufactured using IC-lithography-based etching/dicing techniques to realize microneedle electrode arrays, including circular needles with a diameter of tens of micrometers (i.e., Utah electrode (Hochberg et al. 2006)) or rectangular needles with a cross-sectional area of hundreds of square micrometers (i.e., Michigan electrode (Wise et al. 2004)). Such microneedles consist of one (or several) metal microneedle(s) on each needle as the electrical recording site(s) that detect neural signals. The size of the needle electrode is critical to reduce

the tissue invasiveness and maintain long-term *in vivo* measurements (Geddes and Roeder 2003; Campbell et al. 1991). Kill zones of neurons arise around the surface of the needle electrodes and can be minimized to less than 10 μm by sharpening the electrode tip and smoothing the surface (Edell et al. 1992; Biran et al. 2005; Szarowski et al. 2003; Cheung 2007; Polikov et al. 2005). Very small diameter microneedle implants suppress connective tissue growth due to the tissue response (Geddes and Roeder 2003). Thus, making the tip sharper and the shaft thinner reduces the kill zone associated with tissue penetration. Using a thinner shaft allows higher density microneedle arrays to be realized, which increases the spatial resolution and facilitates the analysis of individual neurons in a network. However, fabrication techniques, such as etching and/or polymer patterning, have limited conventional microneedle arrays to low-density, large shaft diameter arrays.

Even if very small-diameter and high-density electrode arrays can be fabricated, the higher electrical impedance of the electrodes will significantly decrease the signal-to-noise (S/N) ratio. Generally, the area of a metal electrode is equal to that of the electrical double layer between the electrode surface and fluid. In contrast, glass pipette electrodes, which are usually used for intracellular recording, can differentiate these areas because the recording area of these electrodes is determined by the inner diameter of the orifice, and the area of the electrical double layer is defined by the surface area of the inner metal wire. Thus, decreasing the inner orifice diameter and increasing the surface area of the inner metal wire minimize invasiveness and increase the S/N ratio, respectively.

To resolve the issue of high-impedance small-diameter microneedles, we propose integrating high-density sub-5-μm-diameter out-of-plane silicon dioxide (SiO_2) microtube electrode arrays fabricated from silicon (Si) microneedle templates (Fig. 1(a-d)). These arrays are grown by the selective vapor–liquid–solid (VLS) method as described by Takei et al. (2008a). This technique realizes small diameter microtubes that range from a sub-micron to several microns in diameter, which allows high-density tube arrays to be constructed. Figures 1(b–d) show the proposed device and a scanning electron micrograph of a SiO_2 microtube array in which the microtubes are spaced 40 μm apart. In this array, each microtube has a diameter of 3 μm and a length of 40 μm. We have investigated the IC-compatible capability of our drug-delivery microtubes using an n-channel metal oxide semiconductor field effect transistor (NMOSFET) that was manufactured using specific processes at Toyohashi University of Technology, which offers the advantage of on-chip signal processing (Takei et al. 2008b). The mechanical properties of the microtube have also been investigated by using this device for neural recordings (Takei et al. 2008b). However, the electrical properties and recording capability of our device have not been investigated so far. Here, we examined these electrical properties of a microtube and demonstrated the applicability of this device in the electrical *in vivo* recording of evoked neural signals from a rat sciatic nerve.

2 Experimental methods

2.1 Microtube array and packaging

Microtube arrays can be formed with a Si microneedle template, which is fabricated by a selective VLS method at a growth temperature ranging from 500°C to 700°C, and subsequent deposition of SiO_2 over the Si microneedle using plasma enhanced chemical vapor deposition (PECVD) at a deposition rate of 33 $nm \cdot min^{-1}$. The length, diameter, and position of the Si microneedles are controlled by growth time, temperature, and catalytic Au dot size (Takei et al. 2008a; Wagner and Ellis 1964; Park et al. 2008). Thus far, we have achieved a maximum growth rate of 10 $\mu m \cdot min^{-1}$ for the Si microneedle. For the substrates, we used Si (111) substrates with via holes of 40 μm in diameter that were fabricated by deep reactive ion etching (DRIE). After the VLS growth, the Si microneedle is used as a sacrificial structure to form the microtube. The 500 nm wall thickness of the microtube is controlled by the SiO_2 deposition time. Then, SiO_2 at the tip of microneedle was etched by BHF, after which the Au was removed using aqua regia. Finally, the Si microneedle as a sacrificial structure is etched using XeF_2 gas, which has a very high etching selectivity between Si and SiO_2. Various microtubes with inner diameters of 100 nm–6.4 μm have been generated in our laboratory. A more detailed description of the fabrication of microtube arrays was previously reported (Takei et al. 2008a).

Since each microtube electrode requires an individual flexible tube, we designed integrated microchannels using polydimethylsiloxane (PDMS) and flexible tube connectors, resulting in a 500 μm pitch of the active microtube electrode. A PDMS microchannel was fabricated and bonded on the backside of the microtube-fabricated-substrate to connect to each microtube and package the array devices for the first trial. The microchannel was fabricated using a soft lithography technique. A mold Si wafer is prepared using DRIE and coated with fluorocarbon to keep the surface hydrophobic. PDMS was put on the mold wafer and baked at 65°C for 30 min. After the PDMS was cured, it was peeled off the wafer. Finally, the PDMS with microchannel was bonded on the microtube array substrate at a baking temperature of 70°C to withstand desirable flow pressures of 20–45 kPa. Finally, a metal connector was mounted between the PDMS microchannel and a flexible tube connected to a syringe using epoxy.

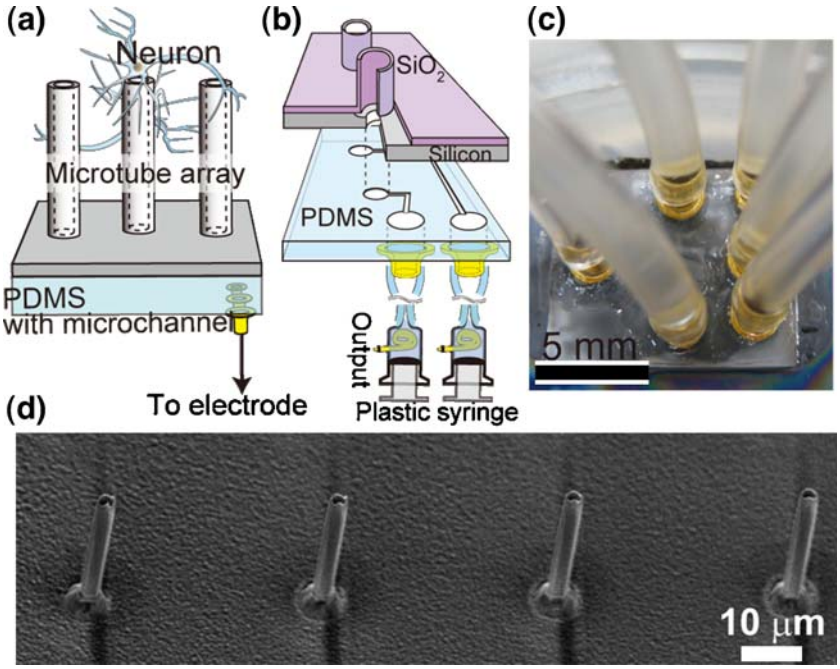

Fig. 1 Proposed methodology for the microtube electrode array. (**a**) A schematic image of the device. (**b**) A schematic of the packaged device. (**c**) A photograph of the packaged device (*backside*). Flexible tubes (Tygon tube) are mounted on PDMS microchannels using metal connectors bonded by glue. (**d**) A SEM image of the microtube electrode array. Microtubes had a 3 μm inner diameter and were 40 μm in length

For electrical measurements of the impedance and test signals, the microtube and the microchannel were filled with a saline solution (resistivity: 14.7 Ω cm) to construct an electrical conductance region to use as an interconnection. We also confirmed that the impedance of an Au wire in a plastic syringe is less than 10 kΩ. To measure the impedance in the saline solution using a silver/silver chloride (Ag-AgCl) electrode as a counter electrode, we used the commercial impedance analyzer at frequency of 500 Hz (Omega-Tip, World Precision Instruments, Inc., USA). To evaluate the effects of capacitances between neighboring microtubes and channels, we used two microtubes with a 500 μm pitch; one (microtube #1) was filled with a saline solution and the other (microtube #2) was filled with a saline (outer)/air gap/saline solution in order to construct an electrically disconnected region in the microtube as shown in Fig. 4(a). Here, we noticed that the saline solution inside microtube electrode #2 was not completely removed. Using the procedure for the test signal recordings, we determined whether there was an air gap inside based on the fact that no signal is recorded when an air gap is in the microtube structure. Test stimulated signals were applied to the saline solution using an Ag-AgCl electrode that was placed approximately 4 cm from the microtube arrays.

2.2 Animal experiments

A male Sprague-Dawley rat (CREA, Japan) weighing 413 g was used to demonstrate the utility of the microtube electrode to record peripheral nerve field potentials. We tested whether evoked potentials could be recorded from the left sciatic nerve with a microtube electrode, as illustrated in Fig. 5(a). All experimental procedures followed the guidelines of the National Institutes of Health of the United States in 1996 and the Japan Neuroscience Society. The institutional committee for animal experiments at the National Institute of Advanced Industrial Science and Technology approved the experimental protocol.

The rat was anesthetized with an intraperitoneal injection of ketamine hydrochloride (75 mg/kg; Sankyo Yell Yakuhin Co., Tokyo, Japan) and xylazine (7.5 mg/kg; Bayer Medical Ltd., Tokyo, Japan). Anesthesia was maintained with supplementary intramuscular injections of ketamine (40 mg/kg) and xylazine (4 mg/kg) every 0.5 to 1 h. The rat was fixed in a stereotaxic frame. The rat's body temperature was maintained at 37°C with a thermostatically regulated heating pad. The skull over the sensorimotor area corresponding to the hindpaw was opened by craniotomy, and then a coaxial electrode (tip: cathode, lateral: anode; IMB-9002-0.5; Inter Medical Co., Ltd., Aichi, Japan) was inserted to a tip depth of 1,600 μm (0.2 mm posterior and 1.8 mm lateral of bregma) to induce flexion of the left ankle with low current electrical stimulation. After the head surgery, the skin over the left leg was opened under local anesthesia. The left biceps femoris muscle was removed and the left sciatic nerve was dissected from the surrounding connective tissue. The sciatic nerve branches, except the tibial nerve branch, were cut.

Then, recording commenced and nerve blockade of action potentials was performed. Figure 5(a) shows the experimental setup. To record field potentials from the sciatic nerve, a fabricated microtube electrode (4.7 μm in inner diameter, 5.7 μm in outer diameter, and 31 μm in length) was placed in the middle of the dissected sciatic nerve, and an Ag-AgCl

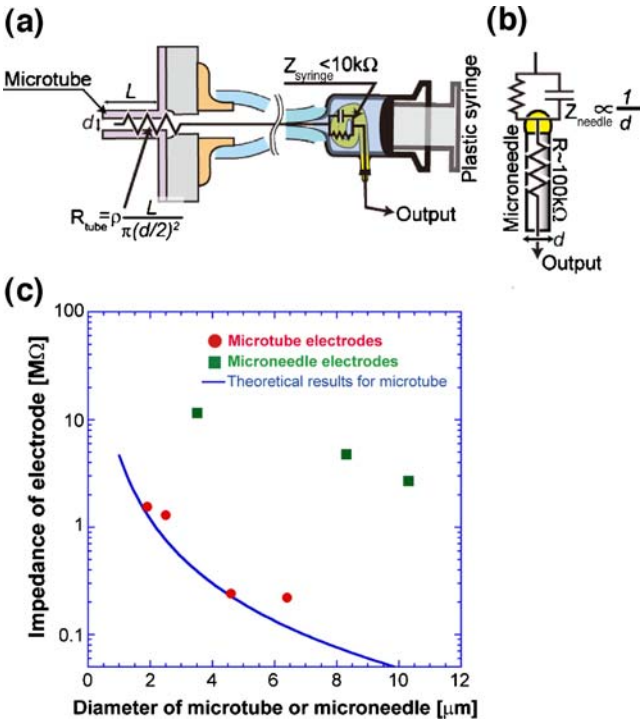

Fig. 2 Electrical impedance of microtube and microneedle electrodes. (**a**) An electrical circuit model for a microtube electrode. (**b**) An electrical circuit model for the previously described microneedle electrode. (**c**) Impedance of microtube and microneedle electrodes at 500 Hz. The *solid line* is the theoretical impedance calculated by the circuit model shown in (**a**)

wire was placed under the peripheral skin as a reference electrode. To simulate a recording condition in which the microtube tips are inserted under the epineurium of a peripheral nerve, the perineurium of the tibial-muscle branch was exposed carefully, and the branch was positioned on a microtube electrode. Nerve field potentials were amplified with a gain of 20,000, band-pass filtered at 500 Hz to 10 kHz, and digitized at 20 kHz. Every 2 s, the sensorimotor cortex was stimulated by a series of three pulses through the coaxial electrode; the pulses were 100 μs in duration and were separated by 20 ms intervals. The evoked potentials of the left anterior tibial muscle were also recorded (gain: 50,000, band-pass filter: 15 Hz to 3 kHz). Nerve blockade was performed during the recording by locally applying a lidocaine solution to the sciatic nerve proximal to the microtube electrode.

3 Results

3.1 Electrical properties of microtube electrodes

We first characterized the electrical impedance of microtube electrodes. Figures 2(a) and (b) compare the microtube electrodes and our previously proposed Si microneedle

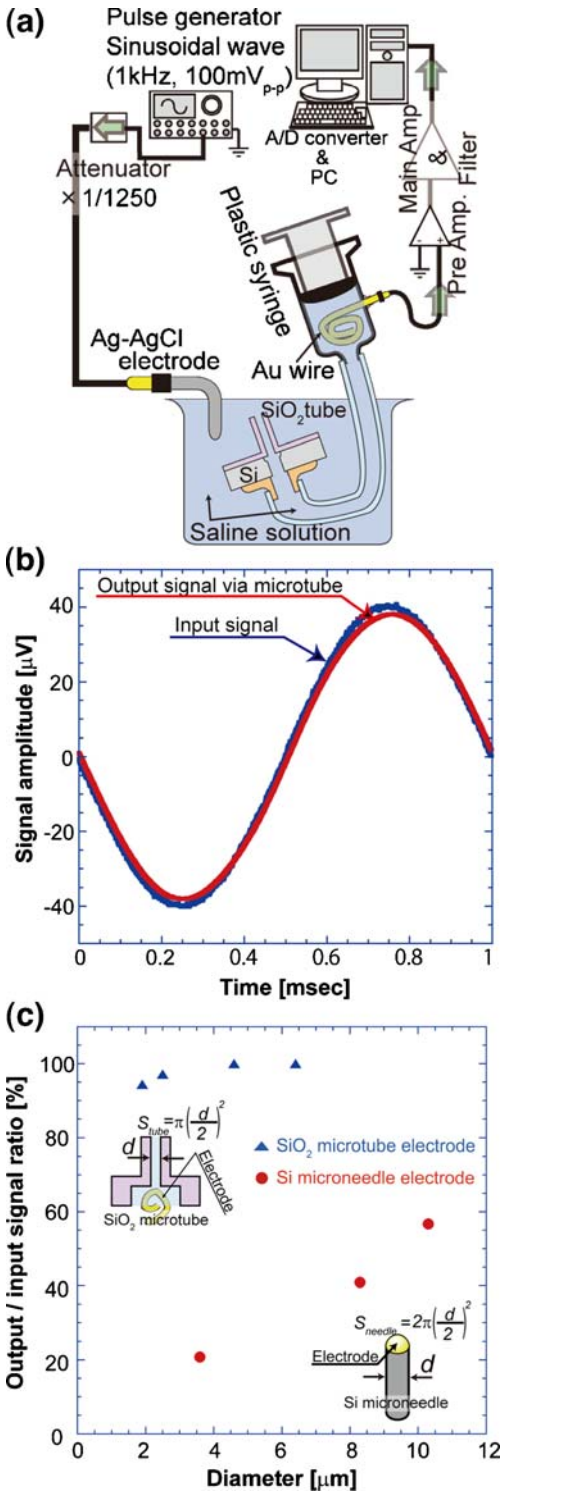

Fig. 3 Test signal recording with microtube electrodes. (**a**) A schematic image of the recording system. (**b**) Input signals and output signals recorded through a 4.6-μm inner diameter microtube electrode. (**c**) Output/input signal ratio recorded with microtube and microneedle electrodes. The recording area of a microneedle electrode, S_{needle}, is larger than that of a microtube electrode, S_{tube}, even when they have the same diameter. However, microtube electrodes have better output/input signal ratios than microneedle electrodes

electrodes using theoretically equivalent circuits for each. The impedance of microtubes with a length of 25 μm and an inner diameter of 1.9, 2.5, 4.6 or 6.4 μm (recording area $\pi(d/2)^2$=2.8, 4.9, 16.6 and 32.2 μm^2) is 1.55, 1.30, 0.24, and 0.22 MΩ, respectively, when measured in saline at 500 Hz using commercial equipment (Omega tip). Thus, as the inner diameter of the microtube increases, the impedance dramatically decreases. These impedance values are much lower than those of Au microneedle electrodes with diameters of 3.5, 8.3 or 10.3 μm (recording area at the hemispherical tips $2\pi(d/2)^2$=19.2, 109.2 and 166.6 μm^2), which have impedances of 11.6, 4.8, and 2.7 MΩ, respectively.

In neural recording systems, signals are attenuated by parasitic impedance associated with the electrode device and the input stage of the recording system. To measure signal attenuation via the microtube electrode, a test sinusoidal signal was applied at 1 kHz into the saline solution via an Ag-AgCl electrode with a distance of approximately 4 cm between the Ag-AgCl electrode and the microtube electrodes (Fig. 3(a)). The output signal through the microtube was detected by an Au wire that was separated from the microtube by a distance of approximately 10 cm. Figure 3(b) shows the input and output curves measured with a 4.6-μm inner diameter microtube electrode. The output/input ratio is close to 100%. Figure 3(c) shows the output results for microtubes with various inner diameters. Microtube electrodes exhibit signal output/input ratios ranging from 94 to 100%, whereas microneedles have signal output/input ratios ranging from 21 to 57% (Fig. 3(c)).

The effects of parasitic capacitances between microtubes and channels should be small for multichannel recording. As shown in Fig. 4(b), microtube #1 detected 100% of the signal output, as described above. However, microtube #2 detected only 4% of the output, indicating that the signal is minimally affected by capacitance from next microtube.

3.2 Recording of nerve field potentials

Nerve field potentials elicited by electrical stimulation of the hindpaw motor cortex were recorded from a rat sciatic nerve using a microtube electrode (Fig. 5(a)). Figure 5(b) shows the integrated-and-rectified nerve field potential (INFP) of the left sciatic nerve and integrated-and-rectified electromyogram (IEMG) of the left anterior tibial muscle evoked by cortical stimulation of the right hindpaw motor area during nerve blockade. The latency of the INFP was shorter than that of the IEMG, indicating that the evoked field potentials traveled through the bundle of sciatic nerves to the muscle. The INFP and IEMG disappeared 31 min after lidocaine was administered to the sciatic nerves proximal to the microtube, and the activity of the sciatic nerves recovered 94 min after the lidocaine administration. The linear correlation between INFPs and IEMGs is shown in Fig. 6.

4 Discussion

We designed a high-density sub-5-μm-diameter microtube electrode array that can be used as a low invasive electric-neural interface device. The microtube structure effectively reduced the electrode impedance relative to that of a microneedle electrode with the same diameter. To verify the utility of the microtube electrodes, we compare both the impedances and signal attenuation ratios between microtube and microneedle electrodes. The signal affected by parasitic capacitances between microtube electrodes was also measured. Finally, the remaining issues and merits of the microtube device are discussed

Our previous VLS-microneedle fabricated electrode array attenuated the signal by at least 40% (Takei et al. 2008b), due to the input impedance of the amplifier and the

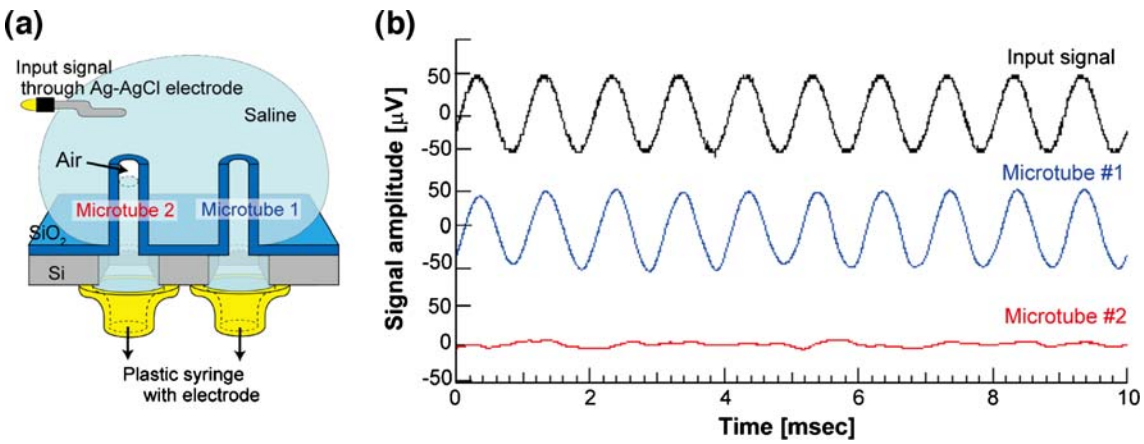

Fig. 4 Effects of parasitic capacitances between neighboring microtubes and channels. (**a**) Experimental setup for recording signal differences between two microtubes. (**b**) Waveforms of input signals and signals derived with microtubes #1 and #2

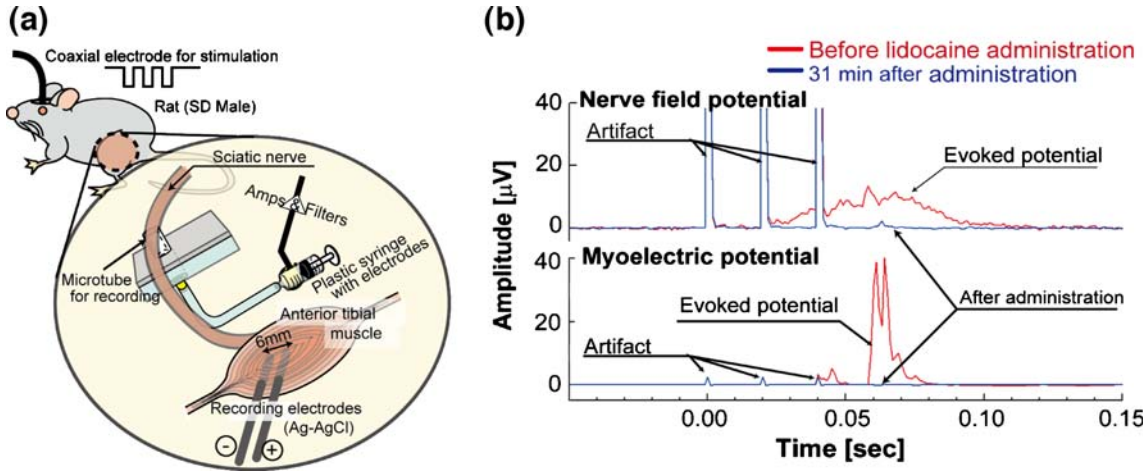

Fig. 5 *In vivo* recording of evoked nerve field potentials from the sciatic nerve. (**a**) Experimental setup. (**b**) Evoked nerve field potentials and myoelectric potentials before and after lidocaine administration. Nerve field potentials from 0.044 s to 0.059 s (after the disappearance of artifacts due to the third stimulation pulse) were integrated as INFP, and myoelectric potentials from 0.059 s to 0.08 s were collected as IEMG. Thus, artifacts were excluded from the INFP and IEMG calculations, and the contamination of INFP and IEMG measurements is minimized

high impedance (>10 MΩ) of sub-5-μm-diameter microneedle electrodes, which generate a voltage dividing circuit. Electrode impedance is inversely proportional to the surface area, and the recording area of the microneedle is only the very small tip region (Fig. 2(b)). We attempted to reduce the electrode impedance using platinum black or other metals and integrating source follower amplifier circuits (Mayumi et al. 2008). However, the structure of such a needle electrode array is very complex and there are many fabrication issues (e.g., the high input impedance of the integrated circuits makes the signal response slow; sodium ions in the fluid attack the insulator layer of integrated circuits, especially that of power lines that have a large voltage difference from the fluid without additional fabrication processes). A high S/N ratio is essential for recording extracellular neural activity and analyzing neural networks because extracellular neural signals are very small in amplitude (i.e., a few hundred microvolts). If signals are attenuated to levels close to the noise level, they become undetectable. It was not feasible to achieve less signal attenuation (high S/N ratio) with the comparable low invasiveness in our previous microneedle electrode system.

Microtube electrode arrays utilize the principles of glass pipette electrodes to realize smaller attenuation and low invasiveness. The impedance of a microtube electrode obeys the theoretical resistance of saline solution and can be calculated using the resistance equation: $R = \rho l/\pi r^2$, where ρ is the resistivity of saline (14.7 Ω cm), l is the length of the microtube (25 μm), and r is the microtube inner radius (1.9–6.4 μm) as shown in Fig. 2(a). Even though the recording area of a microtube electrode is less than 5 μm in diameter, the impedance is less than that of a microneedle electrode with the same diameter (Fig. 2(c)). The signal output/input ratio of the microtube electrode does not significantly change even as the diameter is reduced (Fig. 3(c)), because the impedance is small relative to the input impedance of the amplifier. Therefore, sub-5-μm-diameter microtube electrodes combine a small signal attenuation ratio with low invasiveness without a complex fabrication process.

The signal affected by the capacitances between microtube electrodes is an important consideration when developing high-density microelectrode arrays to record the action potentials of individual neurons and analyze neural networks. This is important because we utilize via holes through the Si wafer as fluidic channels, which could be affected as a path of recorded signal distribution through

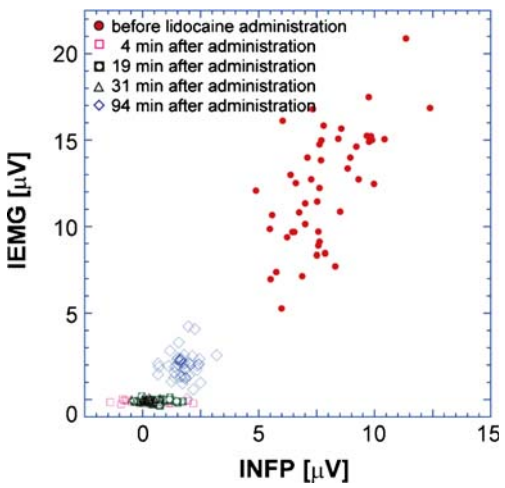

Fig. 6 Correlation between integrated and rectified nerve field potentials (*INFP*) and myoelectric potentials (*IEMG*). See Figure Legend 5 for specifics on the calculation of INFP and IEMG

parasitic capacitances. As expected, the fabricated microtube electrode array does not exhibit significant effects of parasitic capacitances between microtube electrodes. Each microtube electrode minimally affects signals recorded from the next electrode. Microtube #2, which was electrically disconnected from the Ag-AgCl electrode by an air gap preparation, was able to detect the effects of parasitic capacitances between neighboring microtubes and channels. Parasitic capacitances between microtube electrodes underlie the electrical effect on each detected neural signal. However, due to the small capacitance between microtube electrodes, the effect associated with the parasitic capacitance accounts for only 4% of the recorded signal and can consequently be ignored.

To test the neural interface device, a microtube electrode was used for *in vivo* experiments. Neural responses were evoked by stimulating the hindpaw area of the right motor cortex and recorded from the left sciatic nerve via a microtube electrode. To verify the origin of the signal recorded with the microtube, lidocaine (a reversible Na-channel blocker that disrupts the conduction of action potentials) was administered to the sciatic nerve proximal to the microtube electrode to block the nerve. The signals completely disappeared 31 min after the lidocaine injection, but started to recover from the nerve block after approximately 63 min (94 min post lidocaine administration. The fact that the recovered INFP amplitude was 20% compared to the amplitude prior to the nerve block indicates that the recovery was partial and in the early phase). Thus, the signal recorded through the microtube was dependent on sodium channels and was considered to be nerve potentials. The linear relationship between IEMG and INFP shown in Fig. 6 supports this conclusion. Thus, we successfully recorded evoked neural responses using the microtube. Some issues concerning the practical use and implantation of the microtube still remain, such as packaging the device, and future work is necessary to resolve these issues.

Our fabrication method allows for integration with a signal processing circuit. The fabrication method for the microtube array is based on VLS growth of a Si microneedle and subsequent microfabrication techniques. It is not necessary to etch the surface of the Si substrate where the circuits are fabricated. A microtube array for drug-delivery applications has been integrated with on-chip array selectors and source follower amplifiers that were constructed by NMOSFET technology (Takei et al. 2008b). It is necessary to fabricate circuitry on the Si (111) substrate because the VLS-fabricated Si microneedle grows perpendicularly to the (111) substrate. In addition, we have already developed complementary metal oxide semiconductor (CMOS) circuit processes on the Si (111) substrate and have found that the CMOS on Si (111) shares comparable device properties with CMOS on silicon (100), a commonly used substrate in the CMOS industry (Kawano et al. 2004; Takei et al. 2008b; Kato et al. 2004, 2006). However, to realize the fully integrated high-density device, further studies should be conducted, including connecting the inner wall of each microtube to the on-chip circuitry, integrating micropump and microvalves, and realizing microsize tubing and connections (Lee et al. 2007).

The microtube electrode array has several advantages as a neural interface device. The microtube array can function in both electrical recording and drug delivery. The liquid flow properties of the microtube and the ability to deliver drugs to the sciatic nerve *in vivo* have been reported (Takei et al. 2009). The minimal invasiveness of the penetrating microtube array into neural tissues is another advantage. The sub-5-μm-diameter microtube can detect small signals (< 50 μV) in saline without signal attenuation. By comparison, previous sub-5-μm microneedle electrodes have high impedance (10 MΩ), which results in signal attenuation (40%) (Takei et al. 2008b).

5 Conclusions

We designed a high-density, out-of-plane sub-5-μm-diameter microtube electrode array. The microtube electrodes have low impedance and less signal attenuation. In addition, we successfully recorded evoked neural responses from the sciatic nerve. This device has the capacity to become a fully implantable intelligent microchip integrated with signal processing circuits, which can operate as a recording and drug delivery device. We believe our device provides the opportunity to further the study of neuroscience and highlights the importance of future neural interface device applications.

Acknowledgements We thank Mr. M. Ashiki at Toyohashi University of Technology for his assistance with the fabrication process. This work was supported by a grant from the Global COE Program "Frontiers of Intelligent Sensing," a Grant-in-Aid for Scientific Research S (MI), a JSPS fellowship (KT), a CREST project of the Japan Science and Technology Agency (JST) (MI), a grant from the National Institute of Advanced Industrial Science and Technology (HK), and a Strategic Research Program for Brain Sciences (SRPBS) (TK).

References

R. Biran, D.C. Martin, P.A. Tresco, Exp. Neurol. **195**, 115 (2005)
P.K. Campbell, K.E. Jones, R.J. Huber, K.W. Horch, R.A. Normann, IEEE Trans. Biomed. Eng. **38**, 758 (1991)
K.C. Cheung, Biomed Microdevices **9**, 923 (2007)
D.J. Edell, V.V. Toi, V.M. McNeil, L.D. Clark, IEEE Trans. Biomed. Eng. **39**, 635 (1992)
N.A. Fitzsimmons, W. Drake, T.L. Hanson, M.A. Lebedev, M.A.L. Nicolelis, J. Neurosci. **27**, 5593 (2007)

L.A. Geddes, R. Roeder, Ann. Biomed. Eng. **31**, 879 (2003)
L.R. Hochberg, M.D. Serruya, G.M. Friehs, J.A. Mukand, M. Saleh, A.H. Caplan, A. Branner, D. Chen, R.D. Penn, J.P. Donoghue, Nature **442**, 164 (2006)
Y. Kato, H. Takao, K. Sawada, M. Ishida, Jpn. J. Appl. Phys. **43**, 6848 (2004)
Y. Kato, H. Takao, K. Sawada, M. Ishida, Jpn. J. Appl. Phys. **45**, L108 (2006)
T. Kawano, Y. Kato, R. Tani, H. Takao, K. Sawada, M. Ishida, IEEE Trans. Electron Devices **51**, 415 (2004)
S. Kim, R. Bhandari, M. Klein, S. Negi, L. Rieth, P. Tathireddy, M. Toepper, H. Oppermann, F. Solzbacher, Biomed. Microdevices **11**, 453 (2009)
S. Lee, K. Limkrailassiri, Y. Gao, C. Chang, L. Lin, proc. int. conf. microelectromechanical systems (MEMS 2007), p. 61 (2007)
K.A. Ludwig, R.M. Miriani, N.B. Langhals, M.D. Joseph, D.J. Anderson, D.R. Kipke, J. Neurophysiol. **101**, 1679 (2009)
K. Mayumi, K. Takei, T. Kawashima, T. Kawano, H. Takao, K. Sawada, M. Ishida, Proc. Asia-Pacific Conerence of Transducers and Micro-Nano Technology (APCOT 2008), p.113 (2008).
W.I. Park, G. Zheng, X. Jiang, B. Tian, C.M. Lieber, Nano Lett. **8**, 3004 (2008)
V.S. Polikov, P.A. Tresco, W.M. Reichert, J. Neurosci. Methods **148**, 1 (2005)
D.H. Szarowski, M.D. Andersen, S. Retterer, A.J. Spence, M. Isaacson, H. G. Craighead, J.N. Turner, W. Shain, Brain Res. **983**, 23 (2003)
K. Takei, T. Kawashima, K. Sawada, M. Ishida, IEEE Sens. J. **8**, 470 (2008a)
K. Takei, T. Kawashima, T. Kawano, K. Sawada, M. Ishida, J. Micromech. Microeng. **18**, 035033 (2008b)
K. Takei, T. Kawashima, T. Kawano, H. Kaneko, K. Sawada, M. Ishida, Biomed. Microdevices **11**, 539 (2009)
R.S. Wagner, W.C. Ellis, Appl. Phys. Lett. **4**, 89 (1964)
K.D. Wise, J.B. Angell, A. Starr, IEEE Trans. Biomed. Eng. **BME-17**, 238 (1970)
K.D. Wise, D.J. Anderson, J.F. Hetke, D.R. Kipke, K. Najafi, Proc. IEEE **92**, 76 (2004)